

---

# Reverse Redistribution on Exercise-Redistribution $^{201}\text{Tl}$ SPECT in Chronic Ischemic Dysfunction: Predictive of Functional Outcome After Revascularization?

Véronique A. Roelants, MD<sup>1</sup>; Jean-Louis J. Vanoverschelde, MD, PhD<sup>2</sup>; Thierry M. Vander Borgh, MD, PhD<sup>3</sup>; and Jacques A. Melin, MD, PhD<sup>1</sup>

<sup>1</sup>Division of Nuclear Medicine, Cliniques Universitaires St-Luc, Université Catholique de Louvain, Brussels, Belgium; <sup>2</sup>Division of Cardiology, Cliniques Universitaires St-Luc, Université Catholique de Louvain, Brussels, Belgium; and <sup>3</sup>Department of Nuclear Medicine, Mont-Godinne University Hospital, Université Catholique de Louvain, Yvoir, Belgium

---

This study analyzed the incidence and clinical significance of reverse redistribution (RR) on stress-redistribution  $^{201}\text{Tl}$  SPECT studies in patients with poor left ventricular function and tested the hypothesis that the RR phenomenon could be caused by artifacts. **Methods:** Seventy-three consecutive patients with chronic coronary artery disease and left ventricular dysfunction (ejection fraction,  $36\% \pm 12\%$ ) who underwent exercise-redistribution-reinjection  $^{201}\text{Tl}$  SPECT before myocardial revascularization were included. Recovery of left ventricular systolic function was assessed with 2-dimensional echocardiography performed before and  $5.5 \pm 2.5$  mo after revascularization. RR was determined visually and confirmed quantitatively as a  $\geq 10\%$  decrease in  $^{201}\text{Tl}$  uptake on the circumferential profiles. The left ventricle was divided in 16 segments for  $^{201}\text{Tl}$  uptake and wall motion analyses. **Results:** RR was present in 39 of 1,168 segments (3.3%) and in 18 of 73 patients (25%). Before revascularization, regional wall motion was normal in 26 of 39 RR segments (67%), hypokinetic in 7 of 39 (18%), and akinetic in 6 of 39 (15%). Eight percent of all dysfunctional segments (13/167) of RR patients presented RR. After revascularization, 60 of 167 dysfunctional segments (36%) improved function by  $\geq 1$  grade, among which 8 (13%) displayed RR on  $^{201}\text{Tl}$  SPECT before revascularization. Segments with RR improved function more frequently than those without RR (62% vs. 34%;  $P = 0.05$ ). Using a threshold for segmental  $^{201}\text{Tl}$  uptake of  $>54\%$ , the accuracy of  $^{201}\text{Tl}$  reinjection to detect functional improvement in RR segments after revascularization was 77% (10/13). Artificially induced RR was also excluded in all but 1 case because no increased activity of the pixel used for normalization could be found on redistribution images relative to that of the stress images. **Conclusion:** These data suggest that in patients with chronic left ventricular ischemic dysfunction, RR on exercise-redistribution  $^{201}\text{Tl}$  SPECT is not an artifact and occurs rarely in normally functioning and in dysfunctional myocardium. In the latter, RR is frequently associated with myocardial viability

as shown by functional recovery after revascularization. However, the presence or absence of RR in dysfunctional segments seems to be of little clinical relevance.

**Key Words:** reverse redistribution; stress-redistribution-reinjection  $^{201}\text{Tl}$  SPECT; chronic left ventricular dysfunction; myocardial viability

**J Nucl Med 2002; 43:621–627**

---

**R**everse redistribution (RR) is defined as the worsening of a perfusion defect or as the appearance of a new perfusion defect on redistribution images of  $^{201}\text{Tl}$  scintigraphy. RR is found in various clinical conditions and using different imaging protocols. In recent myocardial infarction, RR has been reported on rest-redistribution planar (1) or SPECT (2) imaging, in exercise-redistribution planar (3) and SPECT imaging (4), and, recently, on exercise-redistribution SPECT studies in patients treated with angioplasty (5). In patients with chronic stable coronary artery disease (CAD), RR has been revealed by planar and SPECT imaging techniques during the redistribution phase of rest and stress studies (6–11) as well as after reinjection during a stress-redistribution-reinjection planar protocol (12). The RR phenomenon has also been shown in other various clinical situations, such as sarcoidosis (13), chronic Chagas disease (14), Wolff-Parkinson-White syndrome (15), Kawasaki disease (16), syndrome X (17), after heart transplantation (18), and even after dipyridamole perfusion in healthy patients (19).

The clinical significance of RR on stress-redistribution  $^{201}\text{Tl}$  SPECT in patients with chronic CAD is still incompletely understood. Marin-Neto et al. (7) found that most segments with RR corresponded to viable myocardium on the basis of FDG criteria, adequately diagnosed by  $^{201}\text{Tl}$  reinjection. Similar results have been reported by Soufer et al. (6). However, these data suggesting viability in RR

---

Received May 11, 2001; revision accepted Dec. 4, 2001.  
For correspondence or reprints contact: Véronique A. Roelants, MD, Division of Nuclear Medicine, Cliniques Universitaires St-Luc, Université Catholique de Louvain, Ave. Hippocrate, 10, 1200 Brussels, Belgium.  
E-mail: veronique.roelants@mnuc.ucl.ac.be

segments of CAD patients are based on preserved metabolic activity and, to our knowledge, no previous study has analyzed its significance in terms of functional recovery after revascularization. Therefore, the aim of this study was to determine the incidence and clinical significance of RR on stress-redistribution  $^{201}\text{Tl}$  SPECT for the prediction of functional outcome after revascularization. We also determined the ability of  $^{201}\text{Tl}$  reinjection to differentiate viable from nonviable myocardium in regions with RR and we tested the hypothesis that RR might have been caused by artifacts by an increased activity of the pixel used for normalization on the redistribution images relative to that used for the stress images.

## MATERIALS AND METHODS

### Patient Population

The study group included 73 consecutive patients (62 men, 11 women; age,  $59 \pm 9$  y [mean  $\pm$  SD]; range, 35–74 y) with chronic CAD who were scheduled for coronary revascularization. Some data of our group have been published in a comparison of exercise-redistribution-reinjection  $^{201}\text{Tl}$  SPECT with low-dose dobutamine echocardiography for prediction of the reversibility of chronic left ventricular ischemic dysfunction (20). Patients were eligible for inclusion in this study if they showed severe regional dysfunction in the anatomic distribution of at least 1 significantly narrowed or occluded epicardial artery. Their mean left ventricular ejection fraction (LVEF) was  $36\% \pm 12\%$ , as estimated by radionuclide ventriculography ( $n = 33$ ) or by 2-dimensional (2D) echocardiography ( $n = 40$ ). Fifty patients had a history of myocardial infarction, with the most recent occurring 33 d before inclusion in the study. The decision to revascularize was based on clinical consideration to avoid study bias, and the study protocol was approved by our ethical committee. Bypass surgery was performed on 51 patients, whereas the remaining 22 underwent coronary angioplasty. During revascularization, an attempt was made to revascularize all major branches with  $>70\%$  luminal diameter stenosis. In each case, complete revascularization was achieved without perioperative or periprocedural myocardial infarction (defined as new-onset Q-waves on the electrocardiogram or an increase in plasma cardiac enzyme activity after revascularization).

### Data Acquisition

$^{201}\text{Tl}$  SPECT. All patients performed a symptom-limited multi-step dynamic bicycle exercise test. The initial workload was set at 20 W; exercise intensity was then increased by 20 W each minute until the onset of symptoms or the maximal physical tolerance was reached. At peak exercise, 111 MBq (3 mCi)  $^{201}\text{Tl}$  were injected intravenously, after which the patients continued to exercise for another minute. Within 10 min after completion of the exercise test, SPECT images were acquired on a large-field-of-view gamma camera (Starport 400 AC/T; General Electric, Hölte, Denmark) equipped with a high-resolution, parallel-hole collimator centered on the 73- and 164-keV photopeaks, each with a 20% window. A circular  $180^\circ$  orbit was performed starting from  $40^\circ$  right anterior oblique to  $40^\circ$  left posterior oblique at  $6^\circ$  increments for 30 s each. Redistribution images were obtained 4 h later with 40-s acquisition time per angle. Immediately thereafter, all patients received an additional 37 MBq (1 mCi)  $^{201}\text{Tl}$  and a third set of images was acquired 20–30 min later using the redistribution acquisition protocol.

2D Echocardiography. Echocardiograms were obtained using a 2.5- to 3.5-MHz wide-angle, phased-array transducer with 64 or 96

channels. Images from the parasternal long- and short-axis and apical 4- and 2-chamber views were digitized online (ImageVue; Nova Microsonics, Rochester, NY) under basal conditions. Evaluation of wall motion was performed before (within 1 wk of the  $^{201}\text{Tl}$  study) and  $5.5 \pm 2.5$  mo after revascularization.

Radionuclide Ventriculography. In addition to 2D echocardiography, 33 patients underwent radionuclide ventriculography on the same day. Red blood cells were labeled in vivo 20 min after pyrophosphate injection with 740 MBq (20 mCi) of free  $^{99\text{m}}\text{Tc}$ -pertechnetate. Images from the best septal left anterior oblique projection were obtained at rest with a small-field-of-view camera (Apex 215; Elscint, Haifa, Israel) before and after revascularization. Data were acquired for 250,000 counts per frame at 32 frames per cardiac cycle, with a 5% rate of window tolerance.

### Image Processing and Data Analysis

$^{201}\text{Tl}$  SPECT. Sinograms were reconstructed by filtered back-projection with a Butterworth filter (order, 16; cutoff,  $0.25 \text{ cm}^{-1}$ ); then the slices were reoriented along the 3 standard orthogonal planes (transaxial, sagittal, and coronal). No attenuation or scatter correction was performed.

$^{201}\text{Tl}$  images were visually interpreted (normal, moderate, frank, or complete defect) by an experienced observer, who was unaware of the clinical, echocardiographic, or angiographic characteristics of the patients.

Two 2-pixel-thick short-axis slices (at basal and midventricular levels) and the vertical and longitudinal long-axis slices were analyzed semiquantitatively using circumferential profiles. An operator-defined region of interest was drawn around the left ventricular cavity on each short- and long-axis cross section. Myocardial activity was subdivided into 6 sectors emanating from the center of the left ventricle, beginning at the intersection of the anterior and the septal walls for the short-axis slices and proceeding counterclockwise in equal arcs. Two sectors of the vertical long-axis and of the horizontal long-axis slices were also attributed to the apex so that the segmental analysis matched the 16-myocardial-segment model recommended by the American Society of Echocardiography (21). Within each myocardial sector, the mean count per pixel for the stress, redistribution, and reinjection images was computed.

Similarly to Pace et al. (9,10), RR was defined qualitatively as either the appearance of a new defect on the redistribution images (RR-A pattern) or the worsening of a defect apparent on the poststress images (RR-B pattern). Both patterns had to be confirmed quantitatively by a  $\geq 10\%$  decrease on the corresponding circumferential profile, with a relative uptake of  $\geq 80\%$  considered as normal (Fig. 1).

RR was considered to be a potential artifact if, on a short-axis slice where RR was observed, we found another segment with a  $>10\%$  increase of relative uptake on the redistribution study compared with that on the poststress study.

On the basis of our previous experience with exercise-redistribution-reinjection  $^{201}\text{Tl}$  SPECT for prediction of functional outcome after revascularization, the presence of myocardial viability on  $^{201}\text{Tl}$  SPECT was defined as  $>54\%$   $^{201}\text{Tl}$  uptake on reinjection images (20).

2D Echocardiography. Images were interpreted qualitatively by an experienced observer, who was unaware of the scintigraphic, angiographic, and clinical data. Regional function was graded as normal, hypokinetic, or akinetic. Normal wall motion was defined as  $\geq 5$  mm of endocardial excursion and obvious systolic wall thickening, hypokinesia was defined as  $<5$  mm of endocardial

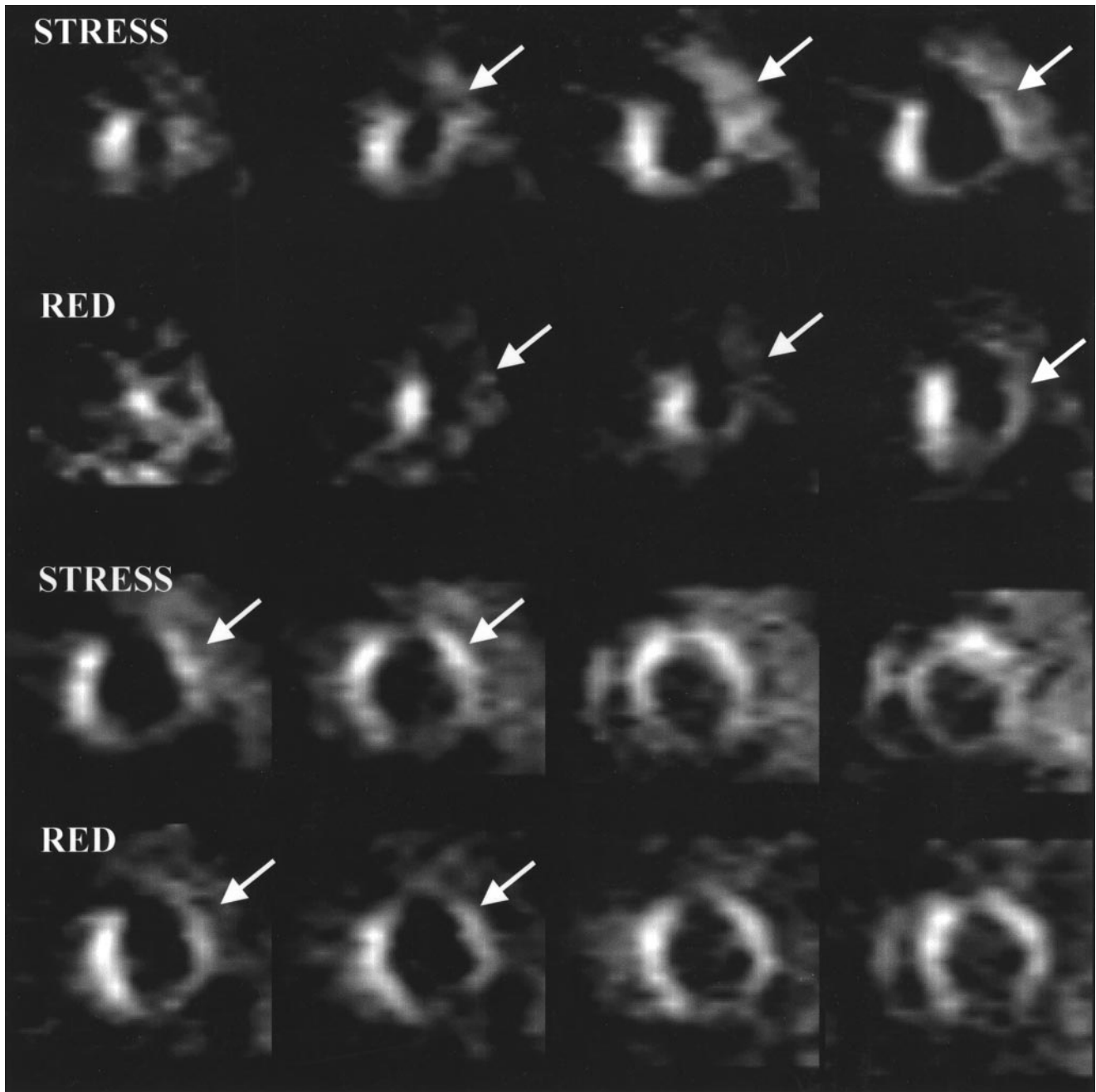


**FIGURE 1.** Stress-redistribution  $^{201}\text{Tl}$  SPECT: short-axis slices from apex (upper left corner) to base (lower right corner). Arrows indicate regions where RR can be observed (i.e., lateral wall). RED = redistribution.

excursion and reduced wall thickening, and akinesia was defined as near absence of endocardial excursion or thickening.

Left ventricular volumes at end diastole and end systole were computed using a standard Simpson's method from the apical 2- and 4-chamber views to estimate LVEF. Functional recovery of a dysfunctional segment was present if the echocardiographic wall motion score of 1 segment improved by at least 1 grade after revascularization (from akinetic to hypokinetic or normal function and from hypokinetic to normal function). Inversely, dysfunction was considered to be persistent if the wall motion score did not improve after revascularization.

*Vascular Supply of Analyzed Segments.* The incidence of RR in the different coronary vascular territories was assessed by ascribing the septum, the anteroseptal wall, and the anterior wall to the left anterior descending coronary artery (LAD), the lateral wall to the circumflex coronary artery (CX), and the inferior wall to the right coronary artery (RCA). Because the vascular supply of the apex varies, this was allocated to any other involved territory. If the apex alone was involved, the LAD was imputed. Likewise, the posterior wall was ascribed to either the RCA or CX territory if either was involved. If the posterior wall alone was involved, it was ascribed to the CX.

*Radionuclide Ventriculography.* The LVEF was calculated from the time–activity curves by use of a conventional semiautomatic approach.

### Statistical Analysis

Continuous variables are expressed as the mean  $\pm$  SD. The  $\chi^2$  test was used to assess differences in frequencies. One-way ANOVA with contrast analyses (Scheffé) was used to compare the different groups. The sensitivity, specificity, and accuracy of  $^{201}\text{Tl}$  reinjection for the diagnosis of myocardial viability were obtained in the usual manner.  $P < 0.05$  was considered as statistically significant.

## RESULTS

RR was found in 25% of the patients (18/73) or in 3.3% of all analyzed segments (39/1,168).

### Characteristics of RR Patients

The clinical characteristics of the patients with (RR group) and without RR (non-RR group) are shown in Table 1. All patients had a significant coronary stenosis ( $\geq 50\%$  reduction in luminal diameter) in at least 1 major vessel. A significantly higher proportion of patients in the RR group had a history of myocardial infarction than in the non-RR group (94% vs. 60%;  $P = 0.006$ ). However, the proportion of patent infarct-related arteries was similar in both groups. Thirty-five patients (48%) presented an LVEF of  $< 35\%$ . The RR pattern was observed in 10 of these patients (28%). Patients in the RR group had significantly fewer ischemic segments on  $^{201}\text{Tl}$  stress-redistribution studies than did patients in the non-RR group ( $1.7 \pm 2$  vs.  $3.5 \pm 2.8$ ;  $P = 0.012$ ). Left ventricular dilatation during exercise was ob-

**TABLE 1**  
Characteristics of Patients With and Without RR

Patient characteristics	RR group (n = 18)	Non-RR group (n = 55)	P
Age* (y)	59 $\pm$ 10	59 $\pm$ 9	NS
Sex ratio (M/F)	16/2	48/7	NS
History of MI	17	33	0.006
Patency of infarct-related artery (n)	6	16	NS
Age-predicted maximal HR* (%)	77 $\pm$ 11	81 $\pm$ 13	NS
Maximal exercise workload* (W)	118 $\pm$ 25	122 $\pm$ 36	NS
LVEF* (%)	33 $\pm$ 12	37 $\pm$ 13	NS
Ischemic segments* (n)	1.7 $\pm$ 2	3.5 $\pm$ 2.8	0.012
Diseased vessels			
1	3	12	
2	8	17	
3	7	26	NS
Revascularization procedure			
PTCA	5	17	
CABG	13	38	NS

\*Data are expressed as mean  $\pm$  SD.

NS = not significant; MI = myocardial infarction; HR = heart rate; PTCA = percutaneous transluminal coronary angioplasty; CABG = coronary artery bypass grafting.

**TABLE 2**  
Magnitude of Functional Recovery in Patients  
With and Without RR

Functional recovery	RR group	Non-RR group	P
Wall motion score			
Before	32 $\pm$ 6	32 $\pm$ 6	NS
After	30 $\pm$ 8	29 $\pm$ 8	NS
EF (%)			
Before	33 $\pm$ 12	37 $\pm$ 13	NS
After	38 $\pm$ 13	40 $\pm$ 16	NS
Difference	5 $\pm$ 8	3 $\pm$ 13	NS

Before = before revascularization; NS = not significant; After = after revascularization; EF = ejection fraction.  
Data are expressed as mean  $\pm$  SD.

served in only 2 of the 18 patients in the RR group. As shown in Table 2, the magnitude of left ventricular functional recovery after revascularization did not differ between both groups.

### Relation of RR to Coronary Distribution and Baseline Left Ventricular Function

As summarized in Table 3, RR was present in 11 segments (28%) of the anterior or septal wall (LAD territory), in 16 segments (41%) of the lateral wall (CX territory), and in 12 segments (31%) of the inferior wall (RCA territory). Two-dimensional echocardiography showed a normal wall motion in 26 of the 39 RR segments (67%), hypokinesia in 7 segments (18%), and akinesia in the remaining 6 segments (15%).

### Relation of RR to Quantitative $^{201}\text{Tl}$ Uptake

Table 4 shows  $^{201}\text{Tl}$  relative uptake after stress and redistribution in normal and dysfunctional RR segments, in normal and dysfunctional non-RR segments of the RR group, and in those segments of the non-RR group. The poststress uptake of the non-RR segments of the RR group is significantly higher than that of the non-RR group.  $^{201}\text{Tl}$  uptake after stress in RR segments was significantly higher than that of the non-RR segments and the non-RR group in normal and in dysfunctional regions. The redistribution uptake of  $^{201}\text{Tl}$  in RR segments was lower than that in the

**TABLE 3**  
Distribution of RR Segments According to Vascular  
Territory and Regional Function

Vascular territory	Normokinetic	Hypokinetic	Akinetic	All
LAD	5	2	4	11
CX	13	1	2	16
RCA	8	4	0	12
All	26	7	6	39



**TABLE 4**  
<sup>201</sup>Tl Relative Uptake (%) After Stress and Redistribution (Red) in Normal and Dysfunctional Segments

Segments	RR group								
	RR segments (n = 39)			Non-RR segments (n = 249)			Non-RR group (n = 880)		
	n	Stress	Red	n	Stress	Red	n	Stress	Red
Normal	26	78 ± 9*	61 ± 8	95	66 ± 15†	67 ± 14	355	60 ± 16	65 ± 14
Dysfunctional	13	64 ± 21*	47 ± 17‡	154	50 ± 18	53 ± 17	525	48 ± 19	55 ± 18

\*P < 0.05 vs. non-RR segments and non-RR group.

†P < 0.05 vs. non-RR group.

‡P = 0.05 vs. non-RR segments.

<sup>201</sup>Tl relative uptake data are expressed as mean ± SD. Comparisons without footnote symbols are not significant.

non-RR segments. However, a statistical difference was almost found only for dysfunctional regions.

Semiquantitative analysis of 39 RR segments revealed a relative <sup>201</sup>Tl uptake after stress of ≥80% in 14 segments (38%) and <80% in the remaining 25 segments. Therefore, most RR segments (64%) presented an RR-B pattern. This pattern was present in 11 of the 13 dysfunctional segments (85%).

#### Relation of RR to Functional Outcome

In RR patients, functional recovery was found in 8 of 13 dysfunctional RR segments (62%) in contrast with 52 of 154 dysfunctional segments without RR (34%; P = 0.05). Therefore, the contribution of RR segments in the functional recovery observed after revascularization is minor (8/60 [13%]). In the non-RR group, 210 of 525 segments (40%) showed functional improvement after revascularization. Functional recovery of segments with an RR-B pattern was 64% (7/11).

Using a mean <sup>201</sup>Tl uptake of >54% at reinjection as the criterion for viability, the sensitivity, specificity, and accuracy of <sup>201</sup>Tl for the detection of viable myocardium in RR segments were 87%, 60%, and 77%, respectively. In comparison, these values were 75%, 52%, and 60%, respectively, for the non-RR segments of that group and 72%, 55%, and 62%, respectively, for the non-RR group. The performance of <sup>201</sup>Tl seems to be higher for the RR segments than for the non-RR segments. However, this was not statistically significant (P > 0.05).

In comparison, redistribution was observed in 34 of the 154 dysfunctional segments (22%) of the RR group. The sensitivity, specificity, and accuracy of redistribution for prediction of outcome were 56%, 55%, and 55%, respectively.

<sup>201</sup>Tl relative uptake after stress, redistribution, and reinjection in viable and nonviable RR and non-RR segments of the RR group is shown in Table 5. Reinjection uptakes are significantly different from redistribution uptakes only for viable segments.

#### RR as Artifact

RR was observed on 20 short-axis slices and 5 long-axis slices, each with its own maximum. An artifactual cause of RR could be excluded by qualitative and semiquantitative analysis in all but 1 segment. The pattern was an increase of 11% in the maximum count per pixel between the poststress and the redistribution phase in the middle segment of the septal wall that induced an apparent decrease of 11% in the middle segment of the lateral wall.

#### DISCUSSION

This study shows that, in patients with chronic CAD, the RR phenomenon observed after stress <sup>201</sup>Tl SPECT studies is rare, occurring in a small percentage of patients (25%) and in a minority of segments (3.3%), primarily with normal wall motion as evaluated by 2D echocardiography. The data also indicate that, when RR is present in dysfunctional

**TABLE 5**  
<sup>201</sup>Tl Relative Uptake (%) After Stress, Redistribution (Red), and Reinjection (Reinj) in Viable and Nonviable RR and Non-RR Segments of RR Group

Segments	RR segments				Non-RR segments			
	n	Stress	Red	Reinj	n	Stress	Red	Reinj
Viable	8	69 ± 13	51 ± 12*	62 ± 9	52	57 ± 17	58 ± 15*	62 ± 13
Nonviable	5	55 ± 28	39 ± 23	45 ± 26	102	47 ± 18	50 ± 18	52 ± 17

\*P < 0.05 vs. Reinj.

<sup>201</sup>Tl relative uptake data are expressed as mean ± SD. Comparisons without footnote symbols are not significant.

segments, it is more often associated with functional improvement after revascularization than dysfunctional segments without RR. In addition, viability in dysfunctional segments with RR can be assessed adequately by  $^{201}\text{Tl}$  reinjection. However, taking into account their number, the contribution of RR segments to the improvement of regional function observed after revascularization is minimal. This study also shows that the origin of the RR phenomenon is not artifactual.

The frequency and significance of RR are very different in patients investigated in the acute phase of myocardial infarction than those in patients with an old myocardial infarction and CAD. In the latter, the phenomenon of RR has been reported during the redistribution phase of either a stress- or a rest-redistribution protocol as well as on images obtained after reinjection (6–12). After reinjection, RR seems to be associated with a significant coronary lesion, collateral-dependent dysfunctional myocardium, and preserved tissue viability as defined by a  $^{201}\text{Tl}$  relative uptake of >55% (12). On rest-redistribution planar imaging studies, Pace et al. (9) found that the RR-A pattern was nearly as frequent as the RR-B pattern and was more predictive of functional recovery as shown by wall motion improvement after revascularization. In our study, the RR-B pattern was the most frequent and was associated with a higher incidence of recovery compared with that of the study by Pace et al. (64% vs. 40%). The difference may be related to different acquisition and technique protocols (rest-redistribution vs. stress-redistribution and planar vs. SPECT methods) and, consequently, to a different model for segments analysis. The difference in the studied population could also interfere.

The significance of RR in poststress studies is still under debate. Previous studies showed discordant results regarding the association with the severity of the coronary disease. Hecht et al. (22), whose patients were evaluated for chest pain, and Marin-Neto et al. (7), whose patients had chronic CAD, concluded that RR was a marker of significant CAD; Tanasecu et al. (23) observed that RR segments were supplied by either normal or mildly diseased coronary arteries. Marin-Neto et al. (7) also observed that the RR phenomenon reflected viable myocardium, critically dependent on collateral circulation. Soufer et al. (6) confirmed these results. However, it is noteworthy that none of these investigators used the reversibility of left ventricular dysfunction after revascularization as the gold standard of myocardial viability. Our study shows that dysfunctional regions with RR often improve after revascularization, and the segments showing this improvement can be identified on the basis of  $^{201}\text{Tl}$  reinjection, as we reported earlier for dysfunctional segments without RR (20). Our findings are consistent with those of Pace et al. (9), who used the same gold standard but with a rest-redistribution imaging procedure. However, in contrast with results of previous studies (6–8), we found a higher proportion of segments with a normal wall motion. The reason of that finding is unclear. This may be partially

explained by differences of the semiquantitative model used for segmental analysis and of the studied population.

In a recent study, Sciagra et al. (8) concluded that the detection of RR on rest-redistribution  $^{201}\text{Tl}$  SPECT studies does not add any information to the quantitative analysis of redistribution activity for prediction of recovery of asynergic segments after revascularization. Our data are in complete agreement with these results because at least 1 dysfunctional RR segment was found in only 6 of 18 patients (33%) and represented only 8 of the 60 segments (13%) that improved function after revascularization.

Several mechanisms could contribute to the RR phenomenon. They were recently summarized by Arrighi and Soufer (24). Among them, the possibility that RR can be produced artifactually is important to consider. Interpolative background subtraction of planar imaging may result in overestimation and underestimation of  $^{201}\text{Tl}$  washout and may cause RR when quantitative analysis is performed (25,26). In our study, performed with a tomographic imaging procedure, we have eliminated another possible artifact caused by the relative nature of the tracer uptake information provided by  $^{201}\text{Tl}$  SPECT because we found only 1 segment in which the activity of the segment used for normalization increased from stress to redistribution.

The small number of dysfunctional RR segments may explain the lack of statistical difference between the redistribution uptake of the nonviable RR segments and that of the nonviable non-RR segments of the RR group (Table 4).

## CONCLUSION

Our data confirm that in patients with chronic left ventricular ischemic dysfunction, RR on exercise-redistribution  $^{201}\text{Tl}$  SPECT studies occurs in regions with normal and abnormal wall motion. Viable myocardium, defined as functional recovery after revascularization, is often found in the dysfunctional segments with RR. However, their contribution to the improvement of regional function observed after revascularization is minimal; therefore, the phenomenon seems to be of little clinical relevance. To further improve our understanding of the pathophysiologic RR mechanisms and of the precise role of RR segments in a global functional recovery after revascularization, studies with a larger patient population are warranted.

## REFERENCES

1. Weiss A, Maddahi J, Lew A, et al. Reverse redistribution of  $^{201}\text{Tl}$ : a sign of nontransmural myocardial infarction with patency of the infarct-related coronary artery. *J Am Coll Cardiol*. 1986;7:61–67.
2. Faraggi M, Karila-Cohen D, Brochet E, et al. Relationship between resting  $^{201}\text{Tl}$  reverse redistribution, microvascular perfusion, and functional recovery in acute myocardial infarction. *J Nucl Med*. 2000;41:393–399.
3. Touchstone D, Beller G, Nygaard T, et al. Functional significance of predischarge exercise  $^{201}\text{Tl}$  findings following intravenous streptokinase therapy during acute myocardial infarction. *Am Heart J*. 1988;116:1500–1507.
4. Fukuzawa S, Ozawa S, Nobuyoshi M, et al. Reverse redistribution on  $^{201}\text{Tl}$  SPECT images after reperfusion therapy for acute myocardial infarction: possible mechanism and prognostic implications. *Heart Vessels*. 1992;7:141–147.
5. De Sutter J, Van de Wiele C, Dierckx R, et al. Reverse redistribution on  $^{201}\text{Tl}$

- single-photon emission tomography after primary angioplasty: one-year follow-up. *Eur J Nucl Med*. 1999;26:633–639.
6. Soufer R, Dey H, Lawson A, et al. Relationship between reverse redistribution on planar  $^{201}\text{Tl}$  scintigraphy and regional myocardial viability: a correlative PET study. *J Nucl Med*. 1995;36:180–187.
  7. Marin-Neto J, Dilsizian V, Arrighi J, et al.  $^{201}\text{Tl}$  reinjection demonstrates viable myocardium in regions with reverse redistribution. *Circulation*. 1993;88:1736–1745.
  8. Sciagra R, Pupi A, Pellegri M, et al. Prediction of post revascularization functional recovery of asynergic myocardium using quantitative  $^{201}\text{Tl}$  rest-redistribution tomography: has the reverse redistribution pattern an independent significance? *Eur J Nucl Med*. 1998;25:594–600.
  9. Pace L, Cuocolo A, Marzullo P, et al. Reverse redistribution in resting  $^{201}\text{Tl}$  myocardial scintigraphy in chronic coronary artery disease: an index of myocardial viability. *J Nucl Med*. 1995;36:1968–1973.
  10. Pace L, Cuocolo A, Maurea S, et al. Reverse redistribution in resting  $^{201}\text{Tl}$  myocardial scintigraphy in patients with coronary artery disease: relation to coronary anatomy and ventricular function. *J Nucl Med*. 1993;34:1968–1973.
  11. Marzullo P, Gimelli A, Cuocolo A, et al.  $^{201}\text{Tl}$  reverse redistribution at reinjection imaging correlated with coronary lesion, wall motion abnormality and tissue viability. *J Nucl Med*. 1996;37:735–741.
  12. Pace L, Perrone-Filardi P, Mainenti P, et al. Effects of myocardial revascularization on regional  $^{201}\text{Tl}$  uptake and systolic function in regions with reverse redistribution on tomographic  $^{201}\text{Tl}$  imaging at rest in patients with chronic coronary artery disease. *J Nucl Cardiol*. 1998;5:153–160.
  13. Fields C, Ossorio M, Roy T, et al.  $^{201}\text{Tl}$  scintigraphy in the diagnosis and management of myocardial sarcoidosis. *South Med J*. 1991;83:2339–2342.
  14. Marin-Neto J, Marzullo P, Marcassa C, et al. Myocardial perfusion abnormalities in chronic Chagas disease as detected by  $^{201}\text{Tl}$  scintigraphy. *Am J Cardiol*. 1992;69:781–784.
  15. Nii T, Nakashima Y, Nomoto J, et al. Normalization of reverse redistribution of  $^{201}\text{Tl}$  with procainamide pretreatment in Wolff-Parkinson-White syndrome. *Clin Cardiol*. 1991;14:269–272.
  16. Tsai C, Lee J, Kao C, et al. Kawasaki disease evaluated by two-dimensional echocardiogram and dipyridamole  $^{201}\text{Tl}$  myocardial SPECT. *Nucl Med Commun*. 1997;18:412–418.
  17. Fragasso G, Rossetti E, Dosio F, et al. High prevalence of the  $^{201}\text{Tl}$  reverse redistribution phenomenon in patients with syndrome X. *Eur Heart J*. 1996;17:1482–1487.
  18. Puskas C, Kosch M, Kerber S, et al. Progressive heterogeneity of myocardial perfusion in heart transplant recipients detected by myocardial perfusion SPECT. *J Nucl Med*. 1997;38:760–765.
  19. Popma J, Smitherman T, Walker B, et al. Reverse redistribution of  $^{201}\text{Tl}$  detected by SPECT imaging after dipyridamole in angina pectoris. *Am J Cardiol*. 1990;65:1176–1180.
  20. Vanoverschelde JL, D'Hondt AM, Marwick T, et al. Head-to-head comparison of exercise-redistribution-reinjection  $^{201}\text{Tl}$  single photon emission computed tomography and low dose dobutamine echocardiography for prediction of reversibility of chronic left ventricular ischemic dysfunction. *J Am Coll Cardiol*. 1996;28:432–442.
  21. American Society of Echocardiography Committee on Standards: subcommittee on quantitation of two-dimensional echocardiograms. Recommendations for quantitation of the left ventricle by two-dimensional echocardiography. *J Am Soc Echocardiogr*. 1989;2:58–67.
  22. Hecht S, Hopkins J, Rose J, et al. Reverse redistribution: worsening of  $^{201}\text{Tl}$  myocardial images from exercise to redistribution. *Radiology*. 1981;140:177–181.
  23. Tanasecu D, Berman D, Staniloff H, et al. Apparent worsening of  $^{201}\text{Tl}$  myocardial defects during redistribution [abstract]. *J Nucl Med*. 1979;20:P688.
  24. Arrighi J, Soufer R. Reverse redistribution: is it clinically relevant or a washout [editorial]? *J Nucl Cardiol*. 1998;5:195–201.
  25. Brown K, Benoit L, Clements JP, et al. Fast washout of  $^{201}\text{Tl}$  from area of myocardial infarction: possible artifact of background subtraction. *J Nucl Med*. 1987;28:945–949.
  26. Lear JI, Raff U, Jain R. Reverse and pseudo-redistribution of  $^{201}\text{Tl}$  in healed myocardial infarction and normal and negative  $^{201}\text{Tl}$  washout in ischemia due to background oversubtraction. *Am J Cardiol*. 1988;62:543–550.

